Model Formulation and Predictions for a Pyrotechnically Actuated Pin Puller*

Keith A. Gonthier† and Joseph M. Powers‡

Department of Aerospace and Mechanical Engineering
University of Notre Dame
Notre Dame, Indiana 46556-5637
USA

Abstract

This paper formulates a multi-phase model which is used to predict the dynamic events associated with the combustion of a pyrotechnic charge in the NASA Standard Initiator (NSI) actuated pin puller. The conservation principles are written as a set of ordinary differential equations and solved to determine system performance. Pressure-time predictions obtained with the model are presented for the simulated firing of an NSI into 1) a pin puller device, 2) a 10 cm^3 closed vessel, and 3) an apparatus known as the Dynamic Test Device. The predictions are compared with experiments. The pressure magnitudes and time scales of pressure rise and decay are predicted well by the model.

Introduction

Pyrotechnically actuated devices are used in numerous aerospace applications. Their ability to reliably deliver high pressures (> 7,000 *psi* [48.25 *MPa*]) within short time scales (< 1 *ms*) renders them the tool of choice for such devices as pin pullers, exploding nuts, and cable cutters. In order to better design these devices, an understanding of both the combustion process in the pyrotechnic and how the products of combustion interact with the device is necessary.

In order to quantify this understanding, it is necessary to develop models. Due to many uncertainties in the chemistry of pyrotechnics, simple models have been the preferred choice, *e.g.*, (Razani, *et al.*, 1990), or (Farren, *et al.*, 1986). These models often use chemical equilibrium calculations to predict the composition of the combustion products and often assume that the combustion process consists of a small number of ideal chemical reactions. The reaction rates are typically modeled by a simple expression which is supported by empirical data. The simple models also require that a number of assumptions be made concerning the gas dynamics; typically a well-stirred reactor is simulated. These assumptions generally restrict the validity of the model to regimes near to those for which empirical data is available.

In the current investigation, we have adopted many of these assumptions, and additionally have placed our study in the context of a new multi-phase flow theory (Powers, *et al.*, 1990a,b). The primary advantages of this approach are that this theory offers a rational framework for 1) accounting for systems in which unreacted solids and condensed phase products account for a large fraction of the mass and volume of the total system, and 2) accounting for the transfer of mass, momentum, and energy both within phases and between phases.

Included in this paper are 1) a description of the basic operation of a pin puller device, 2) a complete description of the model including both a formulation of the model in terms of the mass, momentum, and energy principles supplemented by appropriate geometrical and constitutive relations and the mathematical reductions used to refine this model into a form suitable for numerical computations, and 3) model predictions and comparisons with experimental results.

---

* Presented at the Fifth International Conference of the Groupe de Travail de Pyrotechnie, June 6-11, 1993, Strasbourg, France. This study is supported by the NASA Lewis Research Center under Contract Number NAG-1335. Dr. Robert M. Stubbs is the contract monitor.

† Graduate Research Assistant.

‡ Assistant Professor, corresponding author.

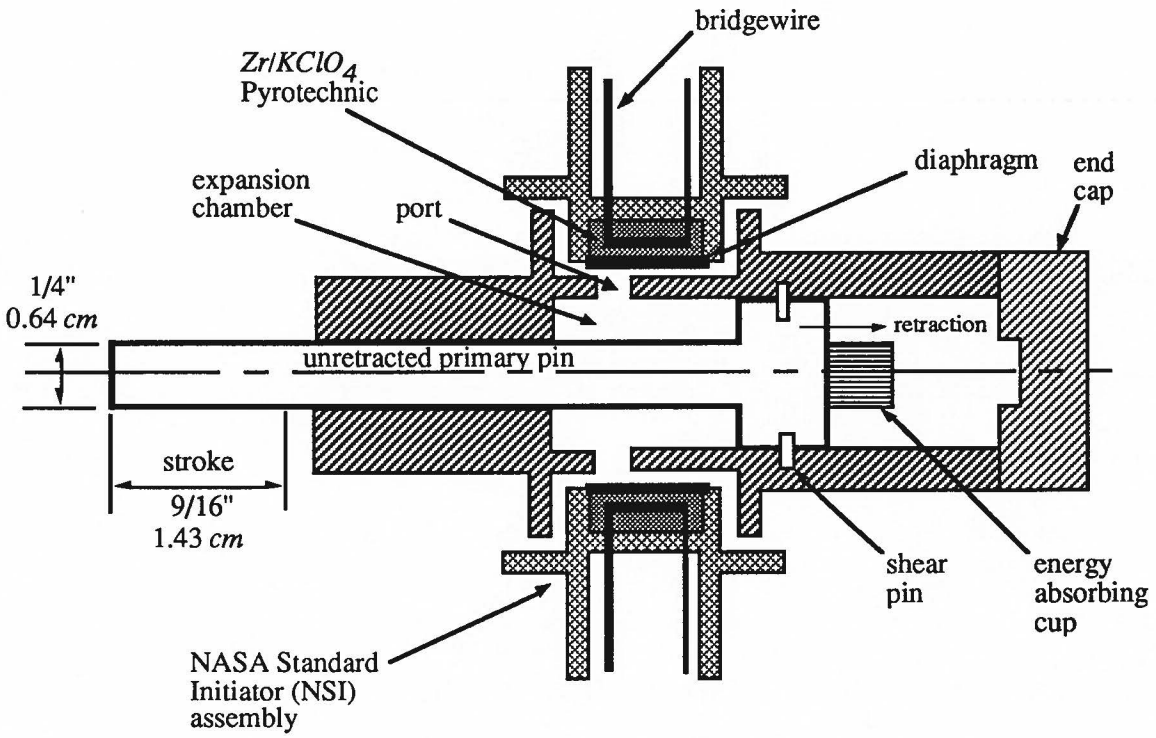

Figure (1). Cross-sectional view of pyrotechnically actuated pin puller.

Basic Operation of Pin Puller

Figure 1 depicts a cross-sectional view of the pyrotechnically actuated pin puller under investigation (Bement, *et al.*, 1991) in its unretracted state.

The primary pin is driven by gas generated by combustion of a pyrotechnic within a device known as the NASA Standard Initiator (NSI). The NSI was originally developed as an initiator for solid rocket motors but has been adapted for other tasks such as this. Two NSI's are threaded into the device's main body. Only one NSI need operate for the proper functioning of the pin puller; the second is a safety precaution in the event of failure of the first. The pyrotechnic consists of a mixture of approximately 114 mg of zirconium fuel (Zr) and potassium perchlorate oxidizer ($KClO_4$). Initially a thin diaphragm tightly encloses the pyrotechnic. Combustion of the pyrotechnic is initiated by the transfer of heat from an electric bridgewire to the pyrotechnic. Upon ignition, the pyrotechnic undergoes rapid chemical reaction producing both condensed phase and gas phase products. The high pressure products accelerate the gas generation rate, burst the confining diaphragm, then vent through the port into the expansion chamber. Should the burst diaphragm block or partially block the port, it is possible for the pin puller to fail to operate properly. Once in the chamber, the high pressure gas first causes shear pins to fail, then pushes the primary pin. After the pin is stopped by crushing an energy absorbing cup, the operation of the device is complete. It is desirable for the energy absorbing cup to absorb a maximum of the kinetic energy of the pin. That portion not absorbed is transmitted in what is known as a "pyrotechnic shock" through the end cap to the supporting structure (*e.g.*, a spacecraft). Peak pressures within the expansion chamber are typically around 7,000 *psi* [48.25 *MPa*]. Completion of the stroke requires about 0.5 *ms*.

Model Description

The model will be presented here in three parts. First, the model assumptions are outlined. Second, the formulation of the model is presented along with the necessary geometrical and constitutive relations. Third, the mathematical reductions are given and the final system of model equations is summarized.

Model Assumptions

Several assumptions were made in formulating the model. For convenience, these assumptions are categorized as fundamental assumptions made in defining the problem, assumptions associated with the combustion process, assumptions associated with mass and heat transfer, and several remaining assumptions used to further simplify the model.

Below, assumptions are listed as main points and the consequences of these assumptions are listed as sub-points.

Fundamental Assumptions

- The total system is a well stirred reactor:
  - there are no spatial variations,
  - all variables are time dependent.
- The total system is modeled as three subsystems: solid pyrotechnic reactants, condensed phase products, and gas phase products.

Combustion Process

- Combustion products are produced in constant ratios which minimize Gibbs free energy:
  - once created, the gas phase mass fractions are frozen,
  - the gas phase combustion products are characterized by a single mixture specific heat and a single mixture gas constant,
- The gas behaves ideally with a temperature dependent specific heat.

Mass and Heat Transfer (see Fig. (2))

- There is no mass exchange between the total system and the surroundings.
- There is a mass exchange from the reactants to both the condensed phase and the gas phase products. The mass exchange rate has been estimated from solid propellant data (Barrere, *et al.*, 1960) and needs to be better estimated for pyrotechnics for which no data has been found.
- There is both heat and work exchange between the total system and the surroundings. The heat exchange is modeled as convective, proportional to the temperature difference, and radiative, proportional to the difference of the fourth power of temperature. The work exchange is due to the volume change induced by the pressure force.
- There is heat exchange between the product subsystems. The rate of exchange is proportional to their temperature difference.
- There is no heat exchange between the reactant subsystem and the product subsystem.
- There is no work exchange between subsystems.

Remaining Assumptions

- The bounding surface of the vessel is isothermal.
- There is no wall friction.
- Both the solid pyrotechnic and the condensed phase products have constant density.
- The kinetic energy of the total system is assumed negligible.
- The kinetic energy of the external pin is non-zero.
- Body forces are assumed negligible.

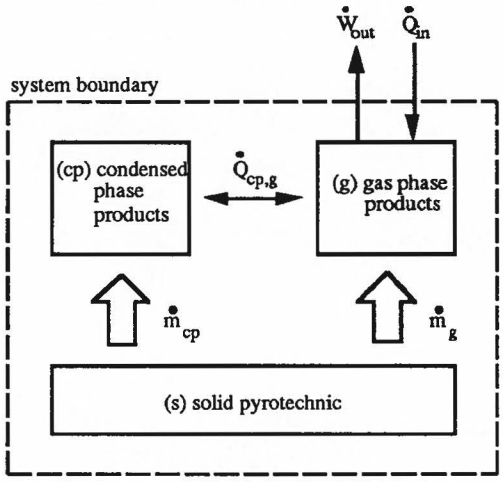

Figure (3). Mass and heat transfer interactions between various subsystems.

Formulation of Non-Dimensional Model

Evolution of mass and energy for each subsystem along with an equation of motion for the pin are written below as a set of non-dimensional ordinary differential equations:

$$\frac{d}{dt}\left[\rho_s V_s\right] = -\rho_s r, \tag{1}$$

$$\frac{d}{dt}\left[\rho_{cp} V_{cp}\right] = \eta_{cp}\rho_s r, \tag{2}$$

$$\frac{d}{dt}\left[\rho_g V_g\right] = \left(1-\eta_{cp}\right)\rho_s r, \tag{3}$$

$$\frac{d}{dt}\left[\rho_s V_s e_s\right] = -\rho_s e_s r, \tag{4}$$

$$\frac{d}{dt}\left[\rho_{cp}V_{cp}e_{cp}\right]=\eta_{cp}\rho_s e_s r-\dot{Q}_{cp,g}, \tag{5}$$

$$\frac{d}{dt}\left[\rho_g V_g e_g\right]=\left(1-\eta_{cp}\right)\rho_s e_s r+\dot{Q}_{in}+\dot{Q}_{cp,g}-\dot{W}_{out}, \tag{6}$$

$$\frac{d^2}{dt^2}\left[z_p\right]=\left[\frac{\tilde{F}_c}{\tilde{m}_p\tilde{V}_c^{1/3}/\tilde{t}_c^{\,2}}\right]F_p. \tag{7}$$

The independent variable of Eqs. (1-7) is time t. The dependent variables are the product gas density ρ_g, the internal energies per unit mass e_s, e_{cp}, e_g, the volumes V_s, V_{cp}, V_g, the pin position z_p, the linear pyrotechnic burn rate r, the rate of heat transfer from the condensed phase products to the gas phase products $\dot{Q}_{cp,g}$, the rate of heat transfer from the surroundings to the system $\dot{Q}_{in}$, the rate of work done by the products in moving the pin $\dot{W}_{out}$, and the net force acting on the pin F_p. The subscript "s" refers to the unreacted solid pyrotechnic mixture, the subscript "cp" refers to the condensed phase combustion products, and the subscript "g" refers to the gas phase combustion products.

Constant parameters are the pin cross-sectional area, which is also the area of the burning surface, $\tilde{A}_p$, the pin mass $\tilde{m}_p$, the unreacted solid pyrotechnic density ρ_s, the condensed phase product density ρ_{cp}, and the mass fraction of the products which are in the condensed phase η_{cp}.

Equations (1-3) describe the evolution of mass of the solid pyrotechnic, condensed phase products, and gas phase products, respectively. Equations (4-6) describe the evolution of energy for the solid pyrotechnic, condensed phase products, and gas phase products, respectively. Equation (7) is the equation of motion for the pin.

Equations (1-7) have been scaled such that all thermodynamic variables and time are $O(1)$ quantities at the completion of the combustion process. Dimensional quantities are indicated by the notation "~". Characteristic scales, denoted by subscript "c", are given by:

$$\tilde{V}_c=\tilde{V}_{so},\qquad \tilde{\rho}_c=\left(1-\eta_{cp}\right)\left(\frac{\tilde{V}_{so}}{\tilde{V}_o}\right)\tilde{\rho}_s,$$

$$\tilde{T}_c=\tilde{T}_{ad},\qquad \tilde{P}_c=\left(1-\eta_{cp}\right)\left(\frac{\tilde{V}_{so}}{\tilde{V}_o}\right)\tilde{\rho}_s\tilde{R}\tilde{T}_{ad},$$

$$\tilde{e}_c=\tilde{e}_{so},\qquad \tilde{F}_c=\tilde{A}_p\left(1-\eta_{cp}\right)\left(\frac{\tilde{V}_{so}}{\tilde{V}_o}\right)\tilde{\rho}_s\tilde{R}\tilde{T}_{ad}, \tag{8}$$

$$\tilde{r}_c=\tilde{b}\left[\left(1-\eta_{cp}\right)\left(\frac{\tilde{V}_{so}}{\tilde{V}_o}\right)\tilde{\rho}_s\tilde{R}\tilde{T}_{ad}\right]^n,$$

$$\tilde{t}_c=\frac{\tilde{V}_{so}}{\tilde{A}_p\tilde{b}\left[\left(1-\eta_{cp}\right)\left(\frac{\tilde{V}_{so}}{\tilde{V}_o}\right)\tilde{\rho}_s\tilde{R}\tilde{T}_{ad}\right]^n}.$$

Additional parameters appearing in Eqs. (8) are the initial solid pyrotechnic volume $\tilde{V}_{so}$, the initial total system volume $\tilde{V}_o$, the adiabatic flame temperature for the reaction $\tilde{T}_{ad}$, the ideal gas constant for the gas phase products $\tilde{R}$, and characteristic burn rate constants $\tilde{b}$ and n.

We model the combustion process by a single irreversible reaction:

$$\sum_{i=1}^{N_s}\upsilon_{s_i}X_{s_i}\longrightarrow\sum_{i=1}^{N_{cp}}\upsilon_{cp_i}X_{cp_i}+\sum_{i=1}^{N_g}\upsilon_{g_i}X_{g_i} \tag{9}$$

where ν_{si}, ν_{cpi}, and ν_{gi} are the stoichiometric coefficients of chemical species X_{si}, X_{cpi}, and X_{gi}, respectively. N_s, N_{cp}, and N_g represent the total number of reactant, condensed phase product, and gas phase product species, respectively. The terms ν_{si} and X_{si} are specified as inputs to the CET89 chemical equilibrium code developed at the NASA Lewis Research Center (Gordon, *et al.*, 1976). The CET89 code determines the products of the reaction and the ratios in which they exists by minimizing the Gibbs free energy. This allows the determination of the mass fraction of products which are in the condensed phase η_{cp}.

Geometric and Constitutive Relations

Appropriate geometrical and constitutive relations necessary to close Eqs. (1-7) are given by the following:

$$V=V_s+V_{cp}+V_g, \tag{10}$$

$$z_p=\left(\frac{\tilde{V}_c^{2/3}}{\tilde{A}_p}\right)V, \tag{11}$$

$$P_g=\rho_g T_g, \tag{12}$$

$$r=r\left(P_g\right)=P_g^n, \tag{13}$$

$$e_s\left(T_s\right)=\sum_{i=1}^{N_s}Y_{s_i}e_{s_i}\left(T_s\right), \tag{14}$$

$$e_{cp}(T_{cp}) = \sum_{i=1}^{N_{cp}} Y_{cp_i} e_{cp_i}(T_{cp}), \quad (15)$$

$$e_g(T_g) = \sum_{i=1}^{N_g} Y_{g_i} e_{g_i}(T_g), \quad (16)$$

$$c_{v_s}(T_s) = \sum_{i=1}^{N_s} Y_{s_i} \frac{d}{dT_s}\left[e_{s_i}(T_s)\right], \quad (17)$$

$$c_{v_{cp}}(T_{cp}) = \sum_{i=1}^{N_{cp}} Y_{cp_i} \frac{d}{dT_{cp}}\left[e_{cp_i}(T_{cp})\right], \quad (18)$$

$$c_{v_g}(T_g) = \sum_{i=1}^{N_g} Y_{g_i} \frac{d}{dT_g}\left[e_{g_i}(T_g)\right], \quad (19)$$

$$\dot{Q}_{cp,g} = \dot{Q}_{cp}(T_{cp}, T_g) = \left[\frac{\tilde{h}_{cp,g}\tilde{T}_c}{\tilde{\rho}_c \tilde{A}_p \tilde{r}_c \tilde{e}_c}\right](T_{cp} - T_g), \quad (20)$$

$$\dot{Q}_{in} = \dot{Q}_{in}(T_g) = \left[\frac{\tilde{h}\tilde{V}_c^{2/3}\tilde{T}_c}{\tilde{\rho}_c \tilde{A}_p \tilde{r}_c \tilde{e}_c}\right] A_w (T_w - T_g) + \left[\frac{\tilde{\sigma}\tilde{V}_c^{2/3}\tilde{T}_c^4}{\tilde{\rho}_c \tilde{A}_p \tilde{r}_c \tilde{e}_c}\right] A_w (\alpha T_w^4 - \varepsilon T_g^4), \quad (21)$$

$$A_w = \left[2\sqrt{\frac{\pi \tilde{V}_c^{2/3}}{\tilde{A}_p}}\right](V - V_s), \quad (21a)$$

$$\dot{W}_{out} = \left[\frac{\tilde{P}_c}{\tilde{\rho}_c \tilde{e}_c}\right] P_g \frac{dV}{dt}, \quad (22)$$

$$F_p = \begin{cases} 0 & \text{if } P_g < F_{crit} \\ P_g & \text{if } P_g \geq F_{crit} \end{cases}. \quad (23)$$

Equations (10) and (11) are geometrical constraints. Here, V is the total volume. Equation (12) is a thermal equation of state for the gas phase combustion products which are assumed to exhibit ideal gas behavior. The pyrotechnic combustion rate r is given by Eq. (13). In this expression, n is an empirically determined constant. This rate is similar in form to those used for solid propellant combustion modeling.

Caloric equations of state for the solid pyrotechnic, condensed phase products, and gas phase products are given by Eqs. (14), (15), and (16), respectively. Here, T_s is the temperature of the solid pyrotechnic and T_{cp} is the temperature of the condensed phase products. Y_{si}, Y_{cpi}, and Y_{gi} are the mass fractions of solid pyrotechnic, condensed phase product, and gas phase product species, respectively. The temperature dependent internal energies for each component of the mixtures are calculated using the CHEMKIN II subroutines and data base developed at Sandia National Laboratories (Kee, *et al.*, 1992). Since for both ideal gases and condensed phase species, the internal energy is only a function of temperature, the specific heat at constant volume for the solid pyrotechnic c_{vs}, the condensed phase products c_{vcp}, and the gas phase products c_{vg} can be obtained via term-by-term differentiation of the above caloric equations of state with respect to their temperature. Expressions for the specific heats at constant volume are given by Eqs. (17), (18), and (19).

Equation (20) gives an expression for the rate of heat transfer from the condensed phase products to the gas phase products. In this expression, $\tilde{h}_{cp,g}$ is a heat transfer coefficient which is assumed to be constant for this study. The heat transfer rate from the gas phase products to the environment, given by Eq. (21), assumes two modes of heat transfer: convective and radiative heat transfer. Parameters in this equation are the convective heat transfer coefficient $\tilde{h}$, the absorptivity of the vessel's walls α, the emissivity of the gas ε, the Stefan-Boltzmann constant $\tilde{\sigma}$, and the vessel's wall temperature T_w. A_w is the instantaneous surface area of the vessel's walls. Equation (21a) relates A_w to V and V_s.

Equation (22) models pressure-volume work done by the expanding gas in moving the pin. Equation (23) models the force acting on the pin due to the gas phase pressure and a restraining force due to the shear pins which are used to initially hold the pin in place. F_{crit} is the critical force necessary to cause shear pin failure. The work associated with shearing the pin is not accounted for.

Mathematical Reductions

In this section, intermediate operations are described which lead to a refined final model. The final model consists of a set of quasi-linear first order ordinary differential equations suitable for numerical integration. To this end, it is necessary to define a new variable $\dot{V}$ to represent the time derivative of total volume:

$$\dot{V} = \left[\frac{\tilde{m}_p \tilde{r}_c^2}{\tilde{P}_c \tilde{V}_c}\right]\frac{dV}{dt}. \quad (24)$$

In these operations, our goal is to write six ordinary differential equations for V, V_S, V_{cp}, T_{cp}, T_g, and $\dot{V}$, and to show how all other variables can be written as functions of these six variables.

First, Eqs. (1), (2), and (3) can be added together to form a homogenous differential equation expressing the conservation of total mass:

$$\frac{d}{dt}\left[\rho_s V_s + \rho_{cp} V_{cp} + \rho_g V_g\right] = 0. \tag{25}$$

Integrating this equation, applying initial conditions which are denoted by the subscript "o", using Eq. (10) to eliminate V_g in favor of V, V_S, and V_{cp}, and solving for ρ_g, it is found that

$$\rho_g\left(V, V_s, V_{cp}\right) = \left[\rho_s V_{so} + \rho_{cp} V_{cpo} + \rho_{go} V_{go} - \rho_s V_s - \rho_{cp} V_{cp}\right] \Big/ \left[V - V_s - V_{cp}\right]. \tag{26}$$

Now, using this expression, Eq. (12) can be used to express P_g as functions of V, V_S, V_{cp}, and T_g:

$$P_g\left(V, V_s, V_{cp}, T_g\right) = \rho_g\left(V, V_s, V_{cp}\right) T_g. \tag{27}$$

With a knowledge of P_g, Eqs. (13) and (23) can be written in the following forms, respectively:

$$r = r\left(V, V_s, V_{cp}, T_g\right) = P_g^n\left(V, V_s, V_{cp}, T_g\right), \tag{28}$$

$$F_p = F_p\left(V, V_s, V_{cp}, T_g\right). \tag{29}$$

We now simplify the remaining mass equations. Since ρ_S and ρ_{cp} are constants, Eqs. (1) and (2) can be rewritten as

$$\frac{dV_s}{dt} = -r\left(V, V_s, V_{cp}, T_g\right), \tag{30}$$

$$\frac{dV_{cp}}{dt} = \eta_{cp}\left(\frac{\rho_s}{\rho_{cp}}\right) r\left(V, V_s, V_{cp}, T_g\right). \tag{31}$$

We now simplify the energy equations. By multiplying Eq. (1) by e_S and subtracting this result from Eq. (4), one determines that

$$\frac{de_s}{dt} = 0. \tag{32}$$

Thus, in accordance with our assumption of no heat transfer to the solid pyrotechnic subsystem, its internal energy remains constant for all time. Integrating, we obtain:

$$e_s = e_{so}. \tag{33}$$

By multiplying Eq. (2) by e_{cp} and subtracting this result from Eq. (5), and by multiplying Eq. (3) by e_g and subtracting this result from Eq. (6), we obtain the following equations, respectively:

$$\rho_{cp} V_{cp} \frac{de_{cp}}{dt} = \eta_{cp}\, \rho_s\, r\left(V, V_s, V_{cp}, T_g\right)\left(e_{so} - e_{cp}\right) - \dot{Q}_{cp,g}\left(T_{cp}, T_g\right), \tag{34}$$

$$\rho_g V_g \frac{de_g}{dt} = \left(1 - \eta_{cp}\right) \rho_s\, r\left(V, V_s, V_{cp}, T_g\right)\left(e_{so} - e_g\right) + \dot{Q}_{cp,g}\left(T_{cp}, T_g\right) + \dot{Q}_{in}\left(T_g\right) - \dot{W}_{out}. \tag{35}$$

Using Eqs. (18) and (19) to re-express the derivatives in terms of T_{cp} and T_g, using the work expression (22) with Eq. (24) to eliminate $\dot{W}_{out}$, expressing all variables as functions of V, V_S, V_{cp}, T_{cp}, T_g, and solving for the derivatives of T_{cp} and T_g, we obtain:

$$\frac{dT_{cp}}{dt} = \left[\eta_{cp}\, \rho_s\, r\left(V, V_s, V_{cp}, T_g\right)\left(e_{so} - e_{cp}\left(T_{cp}\right)\right) - \dot{Q}_{cp,g}\left(T_{cp}, T_g\right)\right] \times \left[\rho_{cp}\, V_{cp}\, c_{v_{cp}}\left(T_{cp}\right)\right]^{-1}, \tag{36}$$

$$\frac{dT_g}{dt} = \left[\left(1 - \eta_{cp}\right) \rho_s\, r\left(V, V_s, V_{cp}, T_g\right)\left(e_{so} - e_g\left(T_g\right)\right) + \dot{Q}_{cp,g}\left(T_{cp}, T_g\right) + \dot{Q}_{in}\left(T_g\right) - \kappa P_g\left(V, V_s, V_{cp}, T_g\right)\dot{V}\right] \times \left[\rho_g\left(V, V_s, V_{cp}\right)\left(V - V_s - V_{cp}\right) c_{v_g}\left(T_g\right)\right]^{-1}. \tag{37}$$

In Eq. (37), κ is a parameter representing the ratio of the rate of work done by the product gases in moving the pin to the rate of energy loss by the solid pyrotechnic due to the combustion process. κ is given by the following expression:

$$\kappa = \left[\frac{\tilde{P}_c^2 \tilde{V}_c}{\tilde{m}_p \tilde{\rho}_c \tilde{e}_c \tilde{r}_c^2}\right]. \tag{38}$$

Final Form of Model Equations

To summarize, the preliminary model can be concisely expressed as an autonomous set of six first order ordinary differential equations in the six variables V, V_S, V_{cp}, T_{cp}, T_g, and $\dot{V}$:

$$\frac{dV}{dt} = \left[\frac{\tilde{P}_c \tilde{V}_c}{\tilde{m}_p \tilde{r}_c^2}\right] \dot{V}, \tag{39}$$

$$\frac{dV_s}{dt} = -r\left(V, V_s, V_{cp}, T_g\right), \tag{40}$$

$$\frac{dV_{cp}}{dt} = \eta_{cp}\left(\frac{\rho_s}{\rho_{cp}}\right) r\left(V, V_s, V_{cp}, T_g\right), \tag{41}$$

$$\frac{dT_{cp}}{dt} = \left[\eta_{cp}\,\rho_s\, r\left(V, V_s, V_{cp}, T_g\right)\left(e_{so} - e_{cp}\left(T_{cp}\right)\right) - \dot{Q}_{cp,g}\left(T_{cp}, T_g\right)\right] \times \left[\rho_{cp}\, V_{cp}\, c_{v_{cp}}\left(T_{cp}\right)\right]^{-1}, \tag{42}$$

$$\frac{dT_g}{dt} = \left[\left(1-\eta_{cp}\right)\rho_s\, r\left(V, V_s, V_{cp}, T_g\right)\left(e_{so} - e_g\left(T_g\right)\right) + \dot{Q}_{cp,g}\left(T_{cp}, T_g\right) + \dot{Q}_{in}\left(T_g\right) - \kappa P_g\left(V, V_s, V_{cp}, T_g\right)\dot{V}\right] \times \left[\rho_g\left(V, V_s, V_{cp}\right)\left(V - V_s - V_{cp}\right) c_{v_g}\left(T_g\right)\right]^{-1}, \tag{43}$$

$$\frac{d\dot{V}}{dt} = F_p. \tag{44}$$

Initial conditions for each of these equations are specified as

$$V(t=0) = V_o, \quad V_s(t=0) = V_{so}, \quad V_{cp}(t=0) = V_{cpo},$$

$$T_{cp}(t=0) = T_o, \quad T_g(t=0) = T_o, \quad \dot{V}(t=0) = 0. \tag{45}$$

All other quantities of interest can be obtained once these equations are solved.

Results

Numerical solutions were obtained for Eqs. (39-44) for the simulated firing of an NSI into the pin puller device. The numerical scheme used was an explicit stiff ordinary differential equation solver given in the standard code LSODE. Also, predicted pressure histories for the simulated firing of an NSI into a 10 cm^3 closed bomb vessel and into the Dynamic Test Device will be presented in order to further corroborate model predictions with available experimental data.

In each of the simulations, the combustion process predicted by the CET89 chemical equilibrium code obeyed the balanced stoichiometric equation presented in Table 1. The parameters chosen are presented in Table 2. These parameters represent preliminary estimates and need to be more carefully chosen based upon the best available data. The initial conditions used are presented in Table 3.

Table 1. Balanced stoichiometric equations used in pyrotechnic combustion simulations.

$$3.7735\,Zr(s) + 2.6917\,KClO_4(s) \longrightarrow$$
$$3.1563\,Zr(cp) + 1.9246\,O(g) + 1.7031\,KCl(g) + 0.9715\,Cl(g) + 0.8590\,K(g) + 0.6309\,O_2(g) + 0.5178\,ZrO_2(g) + 0.1220\,KO(g) + 0.0993\,ZrO(g) + 0.0106\,ClO(g) + 0.0022\,K_2Cl_2(g) + 0.0016\,K_2(g) + 0.0011\,Cl_2(g) + 0.0001\,Zr(g)$$

Table 2. Parameters used in pyrotechnic combustion simulations.

parameter	*value*
$\tilde{A}_p$	0.64^a, 2.0^b, 5.07^c cm^2
$\tilde{\rho}_s$	3.0 g/cm^3
$\tilde{T}_s$	288.0 K
$\tilde{\rho}_{cp}$	1.5 g/cm
h	1.25×10^6 $g/s^3/K$
ε	0.60
α	0.60
$\tilde{h}_{cp,g}$	3.2×10^{10} $g\,cm^2/s^3/K$
$\tilde{F}_{crit}$	3.56×10^7 *dyne* (80 *lbf*)
$\tilde{b}$	0.004 $dyne^{-0.69}cm/s$
n	0.69

(a - pin puller, b - closed bomb, c - Dynamic Test Device)

Table 3. Initial conditions used in pyrotechnic combustion simulations.

initial condition	*value*
V_o	21.69^a, 263.15^b, 32.59^c
V_{so}	1.0
V_{cpo}	8.56×10^{-5}
T_o	5.66×10^{-2}
$\dot{V}_o$	0.0

(a - pin puller, b - closed bomb, c - Dynamic Test Device)

Pin Puller Simulation

Predictions and measurements (Bement, 1992) of pressure time histories for the pin puller are given in Fig. (3). In the experiments, one port contained the NSI and the other a pressure transducer. Here, we predict a rapid pressure rise up to a maximum value near 8,400 *psi* [57.9 *MPa*] occurring about 0.07 *ms* after combustion initiation. Following this maximum, there is a decrease in pressure to a value of 3,500 *psi* [24.13 *MPa*] at completion of the stroke

(0.47 *ms*). We attribute the rapid pressure rise to gases generated during combustion. We attribute the peak pressure to combustion extinction, and the subsequent pressure decay to the combined effect of heat transfer to the surroundings and work done by the expanding gas in moving the pin.

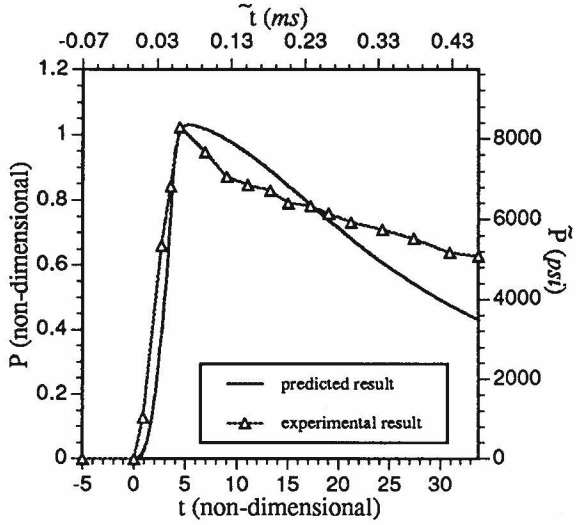

Figure (3). Predicted and experimental pressure histories for the pin puller simulation.

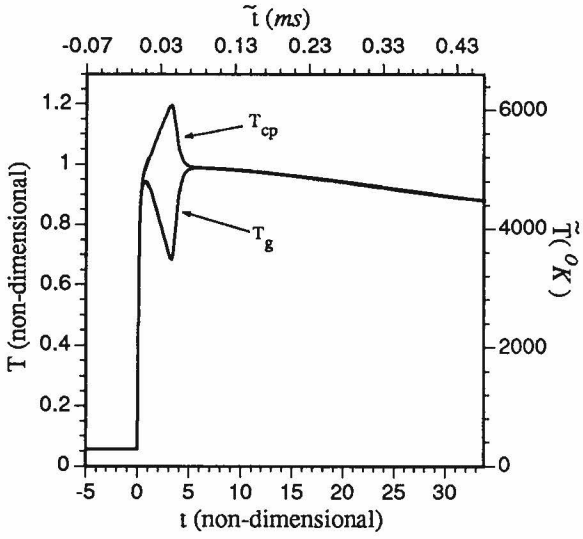

Figure (4). Predicted temperature histories for the pin puller simulation.

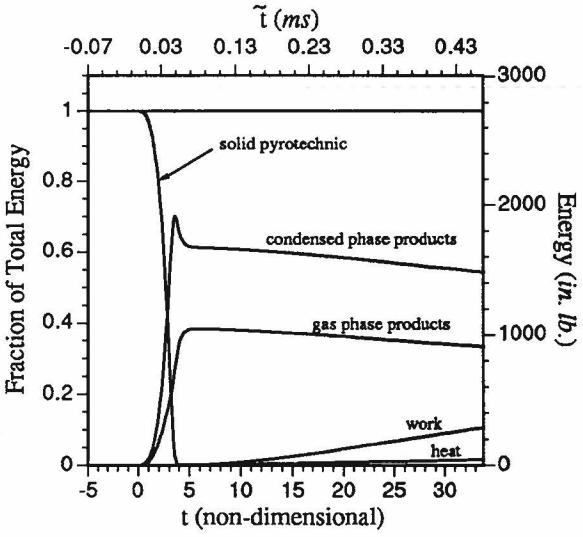

Figure (5). Partitioning of energy for the pin puller simulation.

Figure (4) depicts the predicted temperature histories for both the condensed phase product and gas phase products. Here, we predict a very rapid rise in temperature immediately following combustion initiation. The condensed phase product temperature increases monotonically to a maximum value near 6,100 *K* occurring near the time of combustion extinction. The gas phase products' temperature increases to a local maximum value near 4,600 *K* occurring about 0.005 *ms* after combustion initiation and then decreases to a value near 3,300 *K* at the time of combustion extinction. Following combustion extinction, the two product subsystems thermally equilibrate to a temperature of 4,400 *K* at completion of the stroke. We attribute the increase in temperature of the condensed phase product to its exothermic production from the solid pyrotechnic. Since the rate of gas phase energy production is insufficient to generate a temperature increase, the rise in gas phase product temperature from its initial value to the local maximum is due to heat transfer from the condensed phase product. At the local maximum, the instantaneous rates of gas phase energy production, heat loss to the surroundings, and work done on the surroundings are exactly balanced by the rate of heat transfer from the condensed phase product to the gas phase products. The subsequent decrease in the gas phase product temperature occurs since the rates of gas phase energy production, heat loss to the surroundings, and work done on the surroundings exceed the rate of heat transfer to the gas phase products from the condensed phase product.

Figure (5) illustrates the partitioning of energy between the three subsystems, the kinetic energy of

the pin, and the energy lost to the surroundings as heat. As the combustion proceeds, the energy of the solid pyrotechnic decreases while the energies of both the condensed phase and gas phase products increase. Very little energy is used in moving the pin or lost to the surroundings during this time. Following completion of the combustion process, a larger fraction of the energy is used in retracting the pin. However, for the particular choice of heat transfer parameters used in this study, very little energy is ultimately lost to the surroundings due to heat transfer.

The predicted kinetic energy of the pin at completion of the stroke as indicated in Fig. (5) is 240 *in. lbf* [27 *J*]. Experimentally observed values for the pin kinetic energy at completion of the stroke are typically near 200 *in. lbf* [22.6 *J*].

Closed Bomb Simulation

Closed bomb firings are commonly used as a standard measure of the energy output of pyrotechnic cartridges. In closed bomb testing, a pyrotechnic cartridge is fired into a constant volume bomb and the resulting pressure rise is measured using pressure transducers. A relevant NASA standard states that the firing of an NSI into a 10 cm^3 bomb shall produce a peak pressure of 650 ± 125 *psi* [4.48 ± 0.86 *MPa*] within 5 *ms* (Bement, *et al.*, 1990).

The pressure history predicted by the model is presented in Fig. (6). Also presented in this figure are experimentally observed pressure values (Bement, *et al.*, 1990). Excluding work exchange with the environment, the predicted trends are the same as those presented for the pin puller simulation.

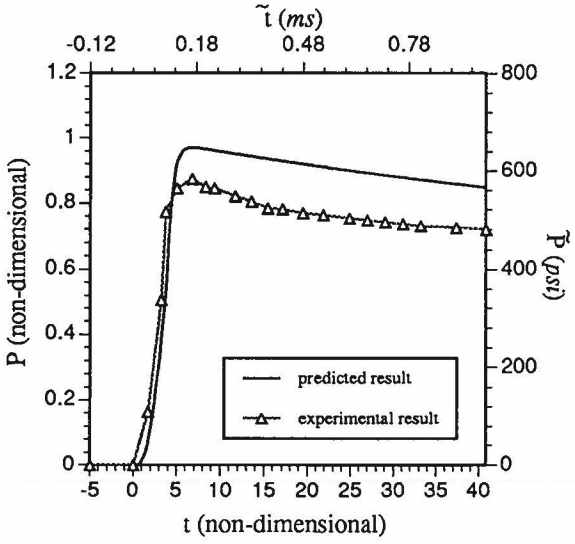

Figure (6). Predicted and experimental pressure histories for the closed bomb simulation.

Dynamic Test Device Simulation

The Dynamic Test Device is a device which was also designed to define and compare the energy production capability of pyrotechnic cartridges. The NSI cartridge output is delivered into a small initial free volume to thrust a one-inch diameter, one-pound mass through a one-inch stroke. The resulting pressure is once again measured with pressure transducers and the energy output is measured as the average kinetic energy of the mass during the stroke.

The predicted and experimental pressure histories are presented in Fig. (7). Experimental values were obtained from (Bement, *et al.*, 1990). The predicted trends are the same as those presented above for the pin puller simulation.

The predicted average kinetic energy of the mass is approximately 391 *in. lbf* [44.2 *J*]. This compares to an experimentally observed value of 258 *in.* lbf. [29.2 *J*].

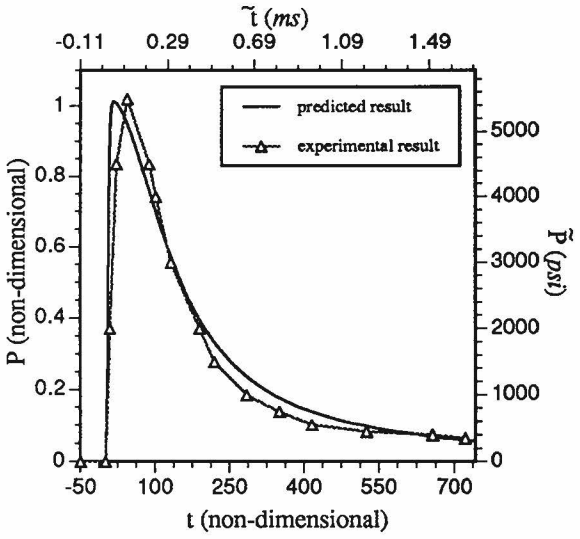

Figure (7). Predicted and experimental pressure histories for the Dynamic Test Device simulation.

Conclusions and Future Work

The model presented in this paper has demonstrated success in predicting the events associated with the firing of pyrotechnically actuated devices. The model correctly predicts time scales and pressure magnitudes. Though the model predicts well variables which are of engineering interest many of the constitutive models are *ad hoc*, though plausible. To better justify our results, we plan to better correlate our constitutive relations with experiments and further to conduct sensitivity

studies for each constitutive model. Additionally, we plan to use the model to study new pyrotechnic formulations.

More advanced studies should relax the assumption of a well-stirred reactor so as to allow for spatial variations. This would allow one to 1) model the important choking phenomena as the combustion products exit the port, 2) better model the interaction between product gases and condensed phase products, 3) include effects of diffusion, 4) include effects of turbulence, and 5) consider non-linear wave dynamics. Such a step would require the solution of a set of partial differential model equations, which significantly complicates the analysis.

Acknowledgment

The authors acknowledge helpful discussions with Prof. P. Barry Butler of the University of Iowa, Iowa City, Iowa, USA.

References

Barrere, M., Jaumotte, A., De Veubeke, B. F., and Vandenkerckhove, J., 1960, *Rocket Propulsion*, Elsevier, New York.

Bement, L. J., 1992, private communication, NASA Langley Research Center, Hampton, Virginia.

Bement, L. J., Multhaup, H. A., and Schimmel, M.L., 1991, "HALOE Gimbal Pyrotechnic Pin Puller Failure Investigation, Redesign, and Qualification," NASA Langley Research Center, Hampton, Virginia.

Bement, L. J., and Schimmel, M. L., 1990, "Cartridge Output Testing: Methods to Overcome Closed Bomb Shortcomings," presented at The 1990 SAFE Symposium, December 11-13, San Antonio, Texas.

Farren, R. E., Shortridge, R. G., and Webster, H. A., III, 1986, "Use of Chemical Equilibrium Calculations to Simulate the Combustion of Various Pyrotechnic Compositions," *Proceedings of the Eleventh International Pyrotechnics Seminar*, pp. 13-40.

Gordon, S., and McBride, B. J., 1976, "Computer Program for Calculation of Complex Chemical Equilibrium Compositions, Rocket Performance, Incident and Reflected Shocks, and Chapman-Jouguet Detonations," NASA SP-273, NASA Lewis Research Center, Cleveland, Ohio.

Kee, R. J., Rupley, F. M., and Miller, J. A., 1992, "CHEMKIN-II: A Fortran Chemical Kinetics Package for the Analysis of Gas Phase Chemical Kinetics," Sandia Report, SAND89-8009B, Sandia National Laboratories, Albuquerque, New Mexico.

Powers, J. M., Stewart, D. S., and Krier, H., 1990a, "Theory of Two-Phase Detonation - Part I: Modeling," *Combustion and Flame*, **80**, pp. 264-279.

Powers, J. M., Stewart, D. S., and Krier, H., 1990b, "Theory of Two-Phase Detonation - Part II: Structure," *Combustion and Flame*, **80**, pp. 280-303.

Razani, A., Shahinpoor, M., and Hingorani-Norenberg, S. L., 1990, "A Semi-Analytical Model for the Pressure-Time History of Granular Pyrotechnic Materials in a Closed System," *Proceedings of the Fifteenth International Pyrotechnics Seminar*, pp. 799-813.